RNA (2000), *6*:1316–1324. Cambridge University Press. Printed in the USA.

Two crystal forms of helix II of *Xenopus laevis* 5S rRNA with a cytosine bulge

YONG XIONG and MUTTAIYA SUNDARALINGAM

The Ohio State University, Biological Macromolecular Structure Center, Departments of Chemistry, Biochemistry and Biophysics Program, Columbus, Ohio 43210, USA

ABSTRACT

The crystal structure of r(GCCACCCUG)•r(CAGGGUCGGC), helix II of the *Xenopus laevis* 5S rRNA with a cytosine bulge (underlined), has been determined in two forms at 2.2 Å (Form I, space group $P4_22_12$, $a = b = 57.15$ Å and $c = 43.54$ Å) and 1.7 Å (Form II, space group $P4_32_12$, $a = b = 32.78$ Å and $c = 102.5$ Å). The helical regions of the nonamers are found in the standard A-RNA conformations and the two forms have an RMS deviation of 0.75 Å. However, the cytosine bulge adopts two significantly different conformations with an RMS deviation of 3.9 Å. In Form I, the cytosine bulge forms an intermolecular C^+∗G•C triple in the *major* groove of a symmetry-related duplex with intermolecular hydrogen bonds between N4C and O6G, and between protonated $N3^+$C and N7G. In contrast, a *minor* groove C∗G•C triple is formed in Form II with intermolecular hydrogen bonds between O2C and N2G, and between N3C and N3G with a water bridge. A partial major groove opening was observed in Form I structure at the bulge site. Two Ca^{2+} ions were found in Form I helix whereas there were none in Form II. The structural comparison of these two forms indicates that bulged residues can adopt a variety of conformations with little perturbation to the global helix structure. This suggests that bulged residues could function as flexible latches in bridging double helical motifs and facilitate the folding of large RNA molecules.

Keywords: 5S rRNA; base triple; cytosine bulge; helix II

INTRODUCTION

The 5S RNA is the smallest ribosomal RNA (rRNA) located at the central protuberance of the large subunit of the ribosome (Shatsky et al., 1980; Stoffler-Meilicke et al., 1981) and plays essential roles in ribosomal functions (Goringer & Wagner, 1986; Meier et al., 1986). The 5S rRNA molecule binds to a number of ribosomal proteins (Huber & Wool, 1984; Dokudovskaya et al., 1996; Green & Noller, 1997) and the protein transcription factor IIIA (TFIIIA), which strongly regulates the transcription of the 5S rRNA gene (Picard & Wegnez, 1979; Pelham & Brown, 1980). In addition to RNA–protein interactions, it has been shown that the 5S rRNA also interacts with other ribosomal RNAs (Chang et al., 1997; Sergiev et al., 1998), indicating its role in the assembly of the ribosome. Since the discovery in 1963 (Rosett & Monier, 1963), 5S rRNA molecules have been subjected to very intensive studies by numerous methods. Currently, about 1,900 5S rRNA genes have been sequenced (Szymanski et al., 1999). Phylogenetic analysis, chemical and enzymatic probing, and computer modeling have yielded a highly conserved secondary-structural model (Fig. 1). However, the three-dimensional structure of 5S rRNA is still eluding the efforts of the RNA community, albeit high resolution structures of a number of 5S rRNA fragments have been determined by X-ray crystallography. These include helix I, a dodecamer duplex encompassing loop E and a 62-nt domain containing helices I and IV and loop E (Betzel et al., 1994; Correll et al., 1997).

The helix II region of 5S rRNA, with a single-nucleotide bulge at a conserved position, has been suggested to interact with a number of proteins. Structural alterations introduced in helix II were shown to interfere with the TFIIIA binding if the changes disrupted the Watson–Crick base paring (Theunissen et al., 1992; McBryant et al., 1995). Helix II is also found to interact with the ribosomal proteins L18 and L25 (Shpanchenko et al., 1996) and its stability influences the association with L18 (Meier et al., 1986). Although the Watson–Crick base pairing is crucial for helix II function, its sequence varies considerably between organisms (Fig. 1). The role of the bulge residue in helix II is not clear in these interactions. However, the fact that it is at a conserved position speaks

Reprint requests to: Muttaiya Sundaralingam, The Ohio State University, Biological Macromolecular Structure Center, Departments of Chemistry, Biochemistry and Biophysics Program, 012 Rightmire Hall, 1060 Carmack Road, Columbus, Ohio 43210, USA; e-mail: sundaral@chemistry.ohio-state.edu.

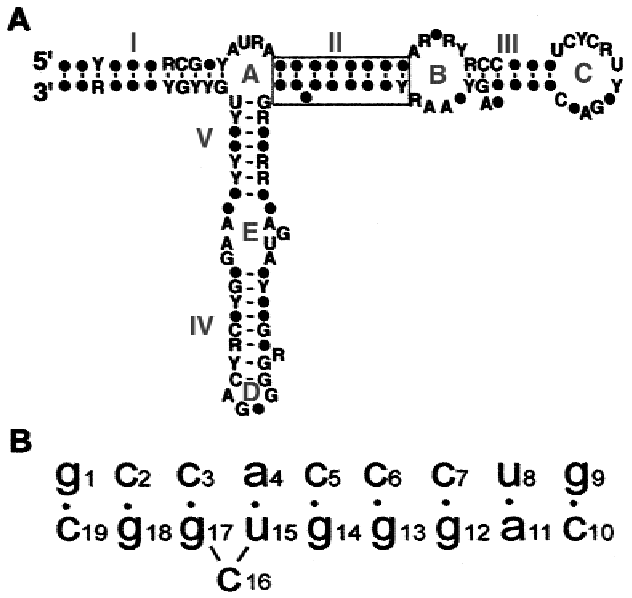

FIGURE 1. **A**: The conserved secondary structure of eukaryotic 5S rRNA (Szymanski et al., 1999). The helix II region studied in this work is boxed. The constant positions are marked with letters (R: purine bases and Y: pyrimidine bases) and variable positions are indicated by dots. Despite variances in sequences, the Watson–Crick pairing is always maintained in the helix II region. **B**: Sequence and numbering scheme of the helix II region studied in this work.

for its importance. The presence of this bulge is highly conserved throughout evolution, and its identity varies with major phylogenetic families. This residue is likely involved in specific 5S rRNA–protein recognition or interaction in prokaryotic and eukaryotic ribosomes (Woese & Gutell, 1989; Zhang et al., 1989).

Bulged residues have been shown to participate in numerous biological functions, including protein–RNA recognition (Wu & Uhlenbeck, 1987; Dingwall et al., 1990), the self-splicing of group II intron and nuclear pre-mRNA (Sharp, 1987), and folding of large RNA molecules (Woese & Gutell, 1989). A single cytosine bulge in the iron responsive element (IRE) RNA is found particularly important in binding of proteins that regulate the iron homeostasis (Jaffrey et al., 1993). These bulged nucleotides might engage in direct contact with proteins and other RNA structural motifs, or play structural roles in recognition by introducing distortion of the RNA helix, thus providing a characteristic shape for binding. High-resolution structural information on single-nucleotide bulges in duplex structures is available for DNA (Joshua-Tor et al., 1992), RNA (Ennifar et al., 1999; Ippolito & Steitz, 2000), chimeric duplex (Portmann et al., 1996), DNA•RNA hybrid (Sudarsanakumar et al., 2000), as well as an RNA–protein complex (Valegard et al., 1997). Structures of RNA duplexes containing multiple-nucleotide bulges are also determined (Ippolito & Steitz, 1998; Wedekind & Mckey, 1999). Interestingly, conformational flexibility seems to be a predominant feature for single-base bulges. Multiple conformations for the bulged residue are found in many crystal structures of oligonucleotide duplexes containing single-nucleotide bulges (Portmann et al., 1996; Ennifar et al., 1999).

In this study, we report the crystal structure of the helix II region of the *Xenopus laevis* 5S rRNA with a cytosine bulge. The cytosine bulge was found in two conformations at 2.2 Å (Form I) and 1.7 Å (Form II). Although the two forms of the bulge have marked differences in conformation and engage in different intermolecular base-triple interactions, the A-form conformation of the helical region is hardly distorted. A partial major groove opening was observed at the bulge site in Form I structure. The results show that the bulge residue can either participate in direct contacts with other molecules via the extrahelical base or introduce a binding site via deforming the local helical region.

RESULTS AND DISCUSSION

The overall conformation of Form I and Form II structures

Both Form I and Form II structures adopt the standard A–RNA conformation for the helical regions (sugar: C3′-endo, base: *anti*, and g^+ for the exocyclic C4′-C5′ bond), while having marked differences in the bulged cytosine residues (Fig. 2). In both forms the bulge assumes an extrahelical position with the flipped-out cytosine base pointing upwards in Form I (Fig. 2A) and pointing downwards in Form II (Fig. 2B). Despite the large deviation in the bulged nucleotides (RMS deviation of 3.9 Å), the helical regions of the two forms have very small variations with an RMS deviation of 0.75 Å (Fig. 2C). The different extrahelical positions of the bulges therefore appear not to affect the A-form geometry of the helical region. The average helical twists are 33.7° and 34.1° for Form I and Form II, respectively, corresponding to 10.7 and 10.6 residues per helical turn, respectively. The minor groove dimensions are uniform in both forms, whereas the Form I helix has a widening of the major groove at the bulge site (discussed in detail in section Major groove widening at the bulge site). The helical axes have very small kinks of ~10° in either form, conforming to other crystallographic studies on single adenosine bulges (Portmann et al., 1996; Ennifar et al., 1999; Sudarsanakumar et al., 2000). Although a kinking angle of this magnitude (~10°) appears insignificant, as it is often found in structures of regular RNA duplexes without a bulged residue, it is consist with the solution estimations of kinking angles (10°–15°) induced by single-nucleotide bulges (Bhattacharyya et al., 1990; Tang & Draper, 1990; Zacharias & Hagerman, 1995). However, a single uracil bulge in the HIV-1 Rev response element (RRE) is found to induce a pronounced kink (~30°) in the helix (Ippolito & Steitz, 2000), although it is not clear to what extent the flank-

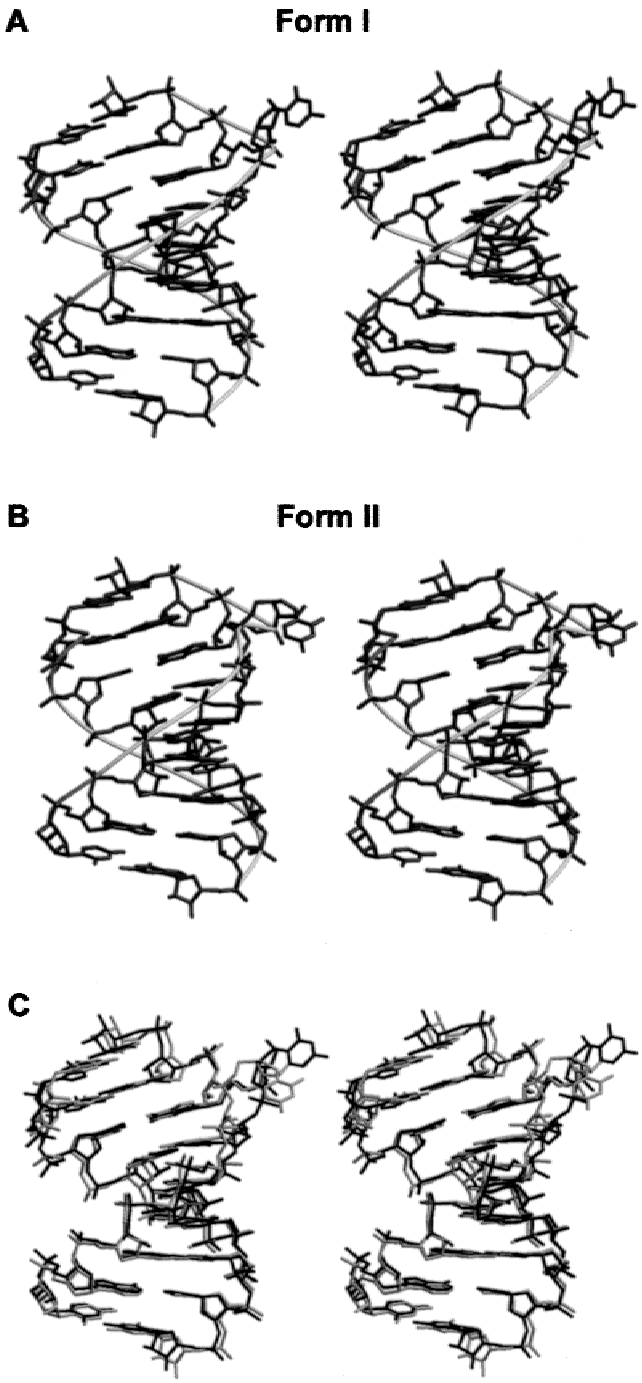

FIGURE 2. A,B: Stereo views of Form I and Form II structures, respectively. The light coils aligning the phosphates illustrate the backbone orientations. **C**: Superposition of Form I (dark) and Form II (light) structures in stereo view. The helical regions of the two forms have an RMS deviation of 0.75 Å; the bulged cytosine residues have an RMS deviation of 3.9 Å.

ing purine•purine mispairs are responsible for that kink, as mispairs are known to cause helix bending (Baeyens et al., 1996; Correll et al., 1997; Pan et al., 1999). Taken together, it appears to enforce the notion that the single-nucleotide bulge acts as a spacer that provides the flexibility to allow the flanking base pairs to orient properly without the restraint of an otherwise continuous helix.

Two conformations of the cytosine bulge emphasize the flexibility of the extrahelical residue

The cytosine C16 in both crystal forms assumes extrahelical positions pointing away from the duplex, with the cytidine base plane almost perpendicular to the base pairs in the helical region (Fig. 2). The cytidine base of the bulge adopts *anti* conformation and the ribose sugar is in C3′-endo puckering mode in both forms, in spite of the flexibility of the bulge. However, C2′-endo sugars were found in structures of most other bulge-containing duplexes (Portmann et al., 1996; Ippolito & Steitz, 1998; Ennifar et al., 1999; Wedekind & Mckey, 1999; Ippolito & Steitz, 2000). Likewise, the *syn* conformation for the bulged base (not necessarily coupled with a C2′-endo sugar) was also found (Portmann et al., 1996; Ennifar et al., 1999; Wedekind & Mckey, 1999). In the present structures, the base and sugar conformations are *anti*/C3′-endo, but the overall structures and orientations of the bulged cytosines exhibit significant differences. In Form I, the C16 bulge is oriented toward the upper part of the molecule, whereas in Form II it takes a sharp turn and flips down toward the lower part. The "up" and "down" conformations for the base were also observed for the adenosine bulge in the structure of Ennifar et al. (1999), where the flip-flop appeared to be linked to changes in the sugar pucker (C3′-endo vs. C2′-endo). The present study shows a C3′-endo sugar in both up and down conformations, indicating such a correlation is not necessary. The differences in orientation of the bulges result in large variations in the sugar–phosphate backbones. The torsion angles $\epsilon/\zeta/\alpha/\beta$ for phosphate group P16 are $-96/-132/57/163$ in Form I, compared to $-147/165/106/-130$ in Form II. The sugar–phosphate backbone at the bulge region functions like a flexible hinge to allow the bulge to adopt a variety of orientations. Water molecules are found to stabilize both bulge backbone conformations via a single water bridge (15O2′···HOH···17O2P) in Form I and two water bridges (15O2P···HOH···16N4 and 15O2P···HOH···16O2P) in Form II. The cytosine bulge conformations in both crystal forms are not related to the catalytic active form for RNA self-cleavage observed in the crystal structures of single-adenosine bulges (Portmann et al., 1996; Sudarsanakumar et al., 2000).

Major groove widening at the bulge site in Form I structure

Although the nonamer length of the duplex does not allow a direct measurement of the major groove width

at the bulge site, it is apparent in Figure 2 that the cytosine bulge C16 in Form I causes the phosphate groups P16 and P17 to move away from the duplex, thus opening up the major groove in this region. It should be noted that this groove widening is different from that caused by kinking of the helical axis, as in the case of the single-adenosine bulge in the chimeric duplex (Portmann et al., 1996); instead it is the result of the direct movement of the sugar–phosphate backbone. This opening of the major groove might render the proximal base edges accessible. More important, the phosphate P16 in Form I shifts about 4 Å outward from its position in the Form II helix, indicating that the backbone of the bulge residue is capable of large movements. Such a large distortion to the backbone could signal a distinctive binding site for the proteins. This might be particularly relevant in helix II of 5S rRNA. The position of this bulge is conserved, but its specific identity varies among species, suggesting that the importance might lie in the structural consequences caused by the presence of a bulge, rather than the nature of the bulged base itself.

Major groove (Form I) and minor groove (Form II) base triples

The bulged cytosine C16 is involved in intermolecular interactions via base-triple formations in both crystal forms (Fig. 3). In Form I, the protonated cytosine C16 forms an intermolecular C^+*G•C base triple in the major groove of a symmetry-related duplex with hydrogen bonds between N4C and O6G and between $N3^+C$ and N7G (Fig. 3B). In addition, the 2′-hydroxyl group of C16 forms an intermolecular hydrogen bond with O1P of G18, further stabilizing this major groove base-triple interaction. Although the pH of the crystallization mixture is about 6, which is well above the pK_a value for protonating N3C, the free-energy gain via the above hydrogen-bonding interactions as well as the base stacking (discussed below) overpower this barrier and drive

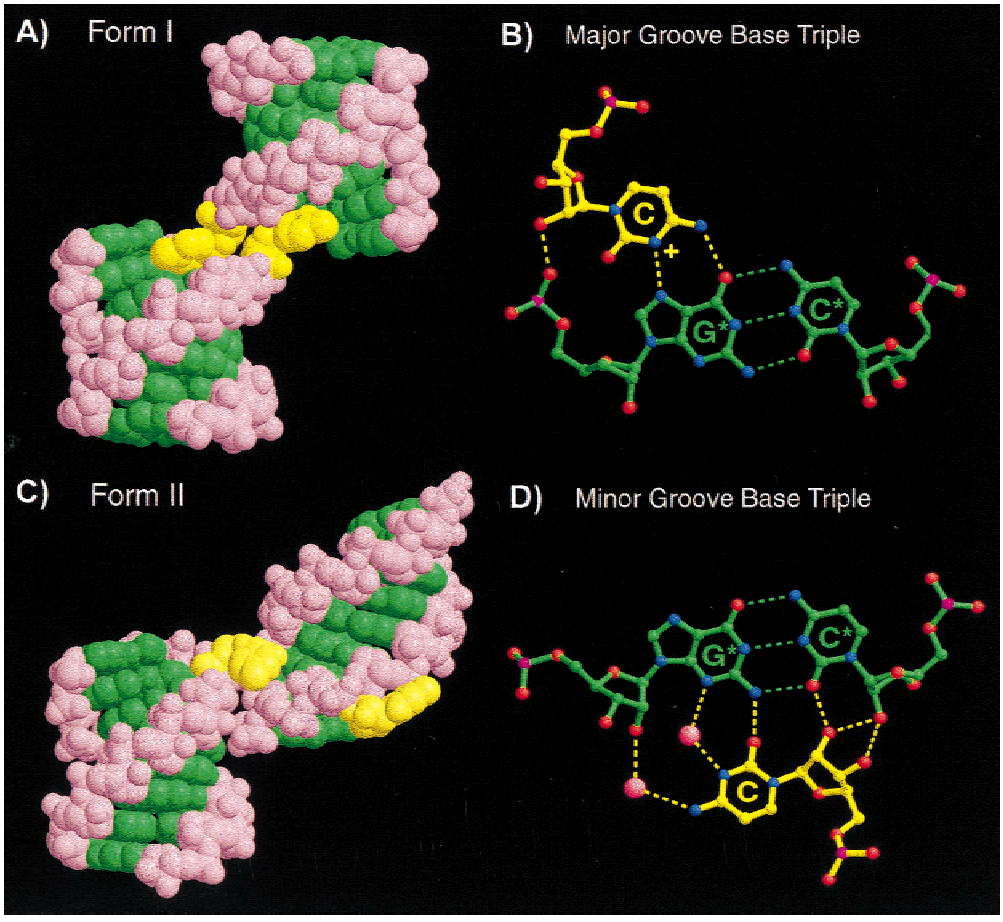

FIGURE 3. Intermolecular base-triple interactions. **A,C**: CPK representations of the intermolecular contacts in Form I and Form II structures, respectively. Base atoms are shown in green, backbones in pink, and the cytosine bulges in yellow. **B,D**: the base-triple hydrogen bonding geometries in the major groove (Form I) and the minor groove (Form II). The large pink balls in **D** represent bridging water molecules.

the base-triple formation. In fact, protonating at a pH above the pK_a value is frequently seen in crystal structures of mispairs (Jang et al., 1998; Pan et al., 1998, 1999). In such cases the crystallization might prove to be facilitated by lowering the pH. In Form II, the bulged C16 approaches a neighboring molecule from the opposite direction, forming a minor groove C*G•C base triple. Extensive hydrogen-bonding interactions occur in the Form II base triple, including direct hydrogen bonding and two water-bridged interactions (Fig. 3D). It is interesting to note that the 2′-OH group of the bulged cytosine is involved in interactions in both forms and further stabilizes the base triples, implying the importance of the 2′-OH group in maintaining three-dimensional RNA structures.

The purine platform in intermolecular interactions

In the Form I structure, besides the intermolecular hydrogen-bonding interactions with G18 in the major groove, the cytosine bulge C16 is engaged in intermolecular base-stacking interactions with the guanosine base G17 (Fig. 4). As the G18 base moves toward the complementary strand and takes part in the interstrand stacking with base C3, it leaves a large portion of the G17 base surface unstacked in the major groove. This exposed base surface functions as a platform on which the incoming C16 lodges. Taken together, guanosine G18 provides the hydrogen-bonding sites to the C16 bulge while guanosine G17 holds the base via stacking interactions. The two consecutive purines therefore work together to lock the incoming base in position. Because the successive purines occur frequently in RNA sequences and the small shift of the upper purine towards the other strand of the duplex exposes the lower purine base surface, the purine platform may be a common interaction motif of three-dimensional RNA molecules.

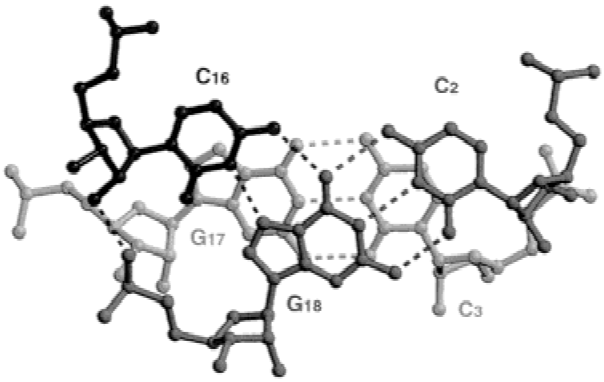

FIGURE 4. The purine platform in the Form I structure. Besides the intermolecular hydrogen bonding interaction with G18, the C16 bulge (black) stacks with an intermolecular residue G17, which acts like a platform to hold the bulge.

Calcium ions participate in intermolecular interactions

Two calcium ions (Ca^{2+}) are identified in the Form I structure. Both of them participate in intermolecular interactions in connecting symmetry-related duplexes (Fig. 5). Surprisingly, no calcium ions were found in the Form II structure, which required a tenfold increase in the calcium ion concentration to crystallize. Ca1 is octahedrally coordinated with six ligands including four phosphate oxygen atoms (symmetry-related 9O1P's) and two water oxygen atoms. It bridges a four-helix junction and sits on a crystallographic 2-fold axis. Ca2 has a coordination number of 7 with distorted pentagonal bipyramid geometry. The direct ligands of Ca2 consist of sugar–phosphate oxygens 19O2′, 19O3′, and 8O1P and four water molecules. The water ligands of Ca2 further contact other symmetry-related duplexes with hydrogen-bonding interactions. Cations are often observed in stabilizing a variety of RNA structural motifs by forming direct interactions or through water interactions with bulges or hairpins (Cate et al., 1997; Correll et al., 1997; Ippolito & Steitz, 1998). In the present structure (Form I), the calcium ions are not located at the bulge site. This may be due to the lack of an intrinsic defined conformation for the single-nucleotide bulge.

Superhelical packing arrangement in Form I crystal

Both crystals pack in the familiar end-to-end pseudo-continuous mode as seen in most RNA crystal structures. However, instead of forming the usual liner columns of the stacked duplexes, which was observed in Form II, a right-handed superhelical packing arrangement is formed in the From I structure (Fig. 6). Two symmetry-related duplexes stack with head-to-head orientation at the junction, creating a virtual twist angle of almost 180° for the junction base pairs. This large twist corresponds to a severe overwinding/unwinding of the duplex in the context of a continuous helix, resulting in the superhelical appearance of the packing. The superhelix contains four nonamer RNA duplexes per superhelical turn with a pitch of 87.0 Å and an outermost diameter of 42.6 Å. Similar superhelical packing patterns have been observed in other crystal structures of RNA oligonucleotides (Portmann et al., 1995; Shi et al., 2000).

Biological implications

In this study we describe the crystal structure of helix II (with a cytosine bulge) of *X. laevis* 5S ribosomal RNA. The three-dimensional structure of the 5S rRNA mol-

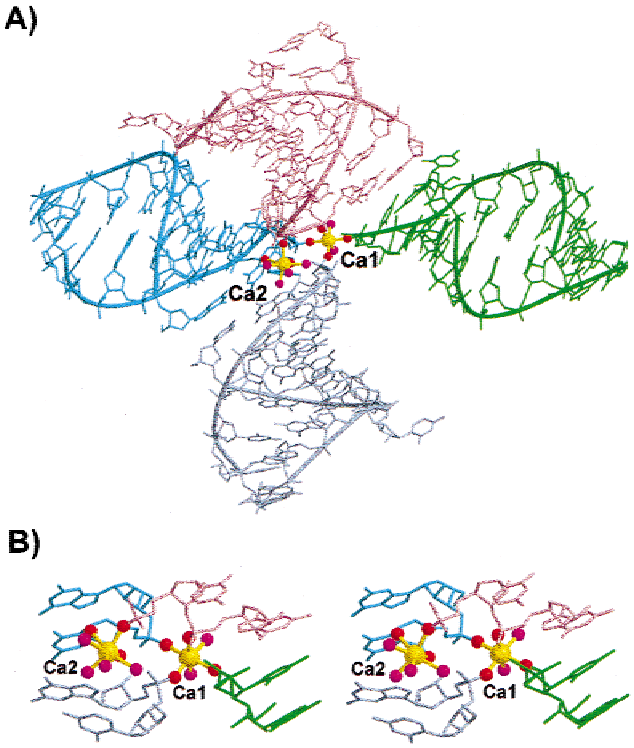

FIGURE 5. **A**: The calcium ions (Ca1 and Ca2, yellow balls) in intermolecular interactions in Form I crystal. The coordinating phosphate/sugar oxygens are shown as red balls and the water ligands as magenta balls. The four symmetry-related duplexes are shown in different colors. The octahedrally coordinated Ca1 sits on a 2-fold axis about 20° to the normal of the plane, and bridges the four-helix junction. Ca2 is in a distorted pentagonal bipyramid geometry. **B**: A close-up look of the calcium binding sites in stereo view.

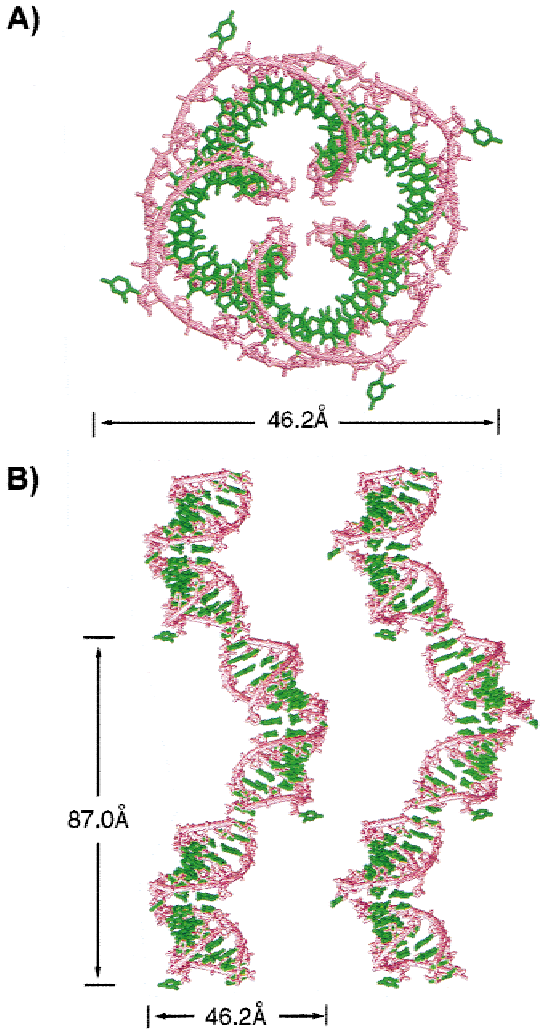

FIGURE 6. The superhelical packing arrangement in Form I crystal. **A**: Top view. **B**: Side view of the right-handed superhelix in stereo. Base atoms are shown in green and backbones in pink.

ecule is still unknown except fragments of helixes I and IV and loop E (Betzel et al., 1994; Correll et al., 1997). We now add to the progress of the structural elucidation of 5S rRNA yet another component, the helix II region. The structural information obtained here could be used to help interpret experimental data acquired by chemical and enzymatic studies as well as in building more precise models.

In eukaryotes, the 5S rRNA molecule is stabilized by the zinc finger protein transcription factor IIIA (TFIIIA) before it incorporates into the ribosome. It has been demonstrated that preserving the helical structure of helix II is critical for TFIIIA binding (Theunissen et al., 1992; McBryant et al., 1995). In this study we observed a regular A-RNA helix with no distinctive structural features associated with the particular sequence of helix II. This is consistent with the above finding that mutations that retain the base pairing in this region do not affect the binding affinity, that is, only a global A-form helical structure is critical. The cytosine bulge is found in extrahelical position with two conformations, and the presence of this flexible bulge has no apparent effect on the global helix. This flexibility would enable the bulge residue to engage in a variety of interactions without disrupting the helix motif, in other words with hardly any cost in free energy. These interactions could involve direct binding to proteins with the extrahelical base, or protein recognition via the opening of the major groove, as observed in the Form I structure, and distortion in the backbones. The latter mechanism has been suggested in a number of RNA–protein interactions, where local distortion of the RNA helix caused by a single-nucleotide bulge is suggested to be more important than the identity of the bulge itself (Jaffrey et al., 1993; Pritchard et al., 1994).

It has been shown that 5S rRNA also interacts with the 23S ribosomal RNA (Sergiev et al., 1998). In the present structures (Form I and Form II) the bulged cytosines are involved in intermolecular interactions via base-triple interactions in both the major and the minor grooves. However, it cannot be implied that these interactions occur between 5S and 23S rRNAs because there is no evidence indicating the association of he-

lix II with 23S rRNA components. Nevertheless, the long-range three-dimensional association via base-triple interaction is known to be an important connecting motif in large RNA molecules. Here we demonstrate bulge residues can participate in the base-triple formation with different configurations (in the major or minor groove), indicating it may function as a flexible latch in bridging helix motifs in RNA structures. The geometry we observed could model and predict the folding of large RNA molecules.

MATERIALS AND METHODS

Synthesis, crystallization, and data collection

The RNA nonamer strand r(GCCACCCUG) and decamer strand r(CAGGGUCGGC) were synthesized using an in-house automated nucleic acid synthesizer (Applied Biosystems, model 391) by the phosphoramidite chemistry. The 2′-hydroxyl groups were deprotected by triethylamine trishydrofluoride (TEA, 3HF) (Westman & Stromberg, 1994) and purified by ion-exchange chromatography. A 1:1 molar ratio of the two strands was mixed at 2 mM concentration in an annealing buffer (5 mM $MgCl_2$, 20 mM sodium cacodylate, pH 6.0). This sample solution was incubated at 65 °C for 15 min and subsequently cooled to room temperature. Crystals were grown at room temperature by the hanging drop vapor diffusion method.

Both forms of the crystals grew only in the presence of calcium ions. Form I crystal was grown by mixing 1 μL of sample solution with 8 μL crystallization buffer containing 20 mM sodium cacodylate (pH 6.0), 5 mM $CaCl_2$ and 5% (v/v) methyl-2,4-pentanediol (MPD) against 1 mL 50% MPD in the reservoir at room temperature. Form II crystals appeared when $CaCl_2$ concentration in the crystallization buffer was increased to 50 mM. Crystal data were collected at Cu Kα radiation (λ = 1.5418 Å) on an in-house Raxis IIc imaging plate system with a Rigaku rotating anode generator. The Form I crystal diffracted to 2.2 Å at −10 °C and it belonged to the tetragonal space group $P4_22_12$ with one duplex in the asymmetric unit. The unit cell constants are $a = b = 57.15$ Å and $c = 43.54$ Å. The Form II crystal diffracted to 1.7 Å at the above temperature and it was indexed in a different tetragonal space group $P4_12_12/P4_32_12$ with cell dimensions of $a = b = 32.78$ Å and $c = 102.5$ Å. There is one duplex in the asymmetric unit. Both crystal data were processed by DENZO and SCALEPACK (Otwinowski & Minor, 1997).

Structure solution and refinement

Form I: The structure was solved by the molecular replacement method using the program package AMoRe (Navaza, 1994) with a nonamer DNA•RNA hybrid duplex (Xiong & Sundaralingam, 1998) as the search model. Correctness of the structure was confirmed by peaks corresponding to the 2′-hydroxyl groups absent from the model DNA strand and a clear indication of the bulged residue in the very first $F_o - F_c$ difference Fourier map. The trial structure was then refined using the program CNS (Brunger et al., 1998). The nucleic acid parameter file dna-rna_rep.param (Parkinson et al., 1996) was used with the dihedral angle restraint released for the bulged cytosine 3′, 5′-diphosphate. Ten percent of the reflections were used for the calculation of R_{free} (Brunger, 1992). Two metal ions with six and seven coordinating ligands involving water oxygens and phosphate oxygens were identified in the $F_o - F_c$ and $3F_o - 2F_c$ electron density maps. Although both Mg^{2+} (annealing buffer) and Ca^{2+} (crystallization buffer) ions were present in the crystallization mixture, the metals were identified as Ca^{2+} ions based on their thermal factors and metal–ligand distances. Because the Ca^{2+} ion has an f″ equal to 1.286 at the Cu Kα wavelength, it provides a unique opportunity to verify its existence by anomalous difference Fourier. The calcium locations were later confirmed by peaks at above 4σ and 5σ, respectively, in the anomalous difference Fourier map, calculated by using anom-

TABLE 1. Crystal data and refinement statistics for Form I and Form II structures.

	Form I	Form II
Space group	Tetragonal $P4_22_12$	Tetragonal $P4_32_12$
Cell parameters		
a (Å)	57.15	32.78
b (Å)	57.15	32.78
c (Å)	43.54	102.51
Volume/base pair (Å^3)	1,871	1,449
Resolution (Å)	2.2	1.7
Unique reflections ($F \geq 2\sigma(F)$)	3,757	6,065
Data completeness (%)	94.8	90.6
R_{merge} (%) on intensity	7.9	7.7
Reflections used	3,704 (10–2.2 Å)	6,022 (10–1.7 Å)
R_{work}	20.4	20.2
R_{free}	22.1	24.3
RMS deviations from ideal geometry		
Parameter file	dna-rna_rep.param	dna-rna_rep.param
Bond lengths (Å)	0.008	0.008
Bond angles (°)	1.3	1.3

alous differences in the Friedel pairs (DANO) as coefficients and phases calculated from the final structure model retarded by 90° (Phi_calc − 90). A total of 23 water molecules were included in the refinement that gave the final R_{work}/R_{free} of 20.4%/22.1% for 3,704 unique reflections ($F > 2\sigma F$) in the resolution range 10–2.2 Å. Data and refinement statistics are summarized in Table 1. The coordinates and the structure factors have been deposited in the Nucleic Acids Database (NDB) and the Protein DataBank (PDB) with access codes AR0026 and 1DQF, respectively.

Form II: The structure was obtained in the space group $P4_32_12$ by the molecular replacement method using the Form I structure as the search model with the bulged cytosine residue not included initially. The refinement procedures were the same as above. Despite a tenfold increase of Ca^{2+} ion concentration used in the crystallization mixture compared to the Form I crystal, there was no calcium ions located in the structure. The anomalous difference Fourier map was featureless, which confirmed the absence of the calcium ion. The final structure included 57 water molecules with a R_{work}/R_{free} of 20.2%/24.3% for 6,022 unique reflections in the resolution range of 10–1.7 Å. Refinement statistics are summarized in Table 1 and the coordinates and structure factors have been deposited in NDB and PDB with access codes AR0027 and 1DQH, respectively.

ACKNOWLEDGMENTS

We acknowledge the support of the National Institutes of Health grant GM-17378 and the Board of Regents of Ohio for an Ohio Eminent Scholar Chair and Endowment to M.S. We also acknowledge the Hays Consortium Investment Fund by the Regions of Ohio for partial support for purchasing the R-axis IIc imaging plate.

Received May 4, 2000; returned for revision May 26, 2000; revised manuscript received June 30, 2000

REFERENCES

Baeyens KJ, De Bondt HL, Pardi A, Holbrook SR. 1996. A curved RNA helix incorporating an internal loop with G.A and A.A non-Watson–Crick base pairing. *Proc Natl Acad Sci USA 93*:12851–12855.

Betzel C, Lorenz S, Furste JP, Bald R, Zhang M, Schneider TR, Wilson KS, Erdmann VA. 1994. Crystal structure of domain A of *Thermus flavus* 5S rRNA and the contribution of water molecules to its structure. *FEBS Lett 351*:159–164.

Bhattacharyya A, Murchie AIH, Lilley DMJ. 1990. RNA bulges and the helical periodicity of double-stranded RNA. *Nature 343*:484–487.

Brunger AT. 1992. The free *R* value: A novel statistical quantity for assessing the accuracy of crystal structures. *Nature 355*:472–474.

Brunger AT, Adams PD, Clore GM, DeLano WL, Gros P, Grosse-Kunstleve RW, Jinag J, Kuszewski J, Nilges M, Pannu NS, Read RJ, Rice LM, Simonson T, Warren GL. 1998. Crystallography and NMR system: A new software suite for macromolecular structure determination. *Acta Cryst D54*:905–921.

Cate JH, Hanna RL, Doudna JA. 1997. A magnesium ion core at the heart of a ribozyme domain. *Nat Struct Biol 4*:553–558.

Chang L-S, Cho Y-C, Lin S-R, Wu B-N, Lin J, Hong E, Sun Y-J, Hsiao C-D. 1997. A novel neurotoxin, cobrotoxin b, from *Naja atra* (Taiwan cobra) venom: Purification, characterization, and gene organization. *J Biochem 122*:1252–1259.

Correll CC, Freeborn B, Moore PB, Steitz TA. 1997. Metals, motifs, and recognition in the crystal structure of a 5S rRNA domain. *Cell 91*:705–712.

Dingwall C, Ernberg I, Gait MJ, Green SM, Heaphy S, Karn J, Lowe AD, Singh M, Skinner. 1990. HIV-1 Tat protein simulates transcription by binding to a U-rich bulge in the stem of the TAR RNA structure. *EMBO J 9*:4145–4153.

Dokudovskaya S, Dontsova O, Shpanchenko O, Bogdanov A, Brimacombe R. 1996. Loop IV of 5S ribosomal RNA has contacts both to domain II and to domain V of the 23S RNA. *RNA*:146–152.

Ennifar E, Yusupov M, Walter P, Marquet R, Ehresmann B, Ehresmann C, Dumas P. 1999. The crystal structure of the dimerization initiation site if genomic HIV-1 RNA reveals an extended duplex with two adenine bulges. *Structure 7*:1439–1449.

Huber PW, Wool IG. 1984. Nuclease protection analysis of ribonucleoprotein complexes: Use of the cytotoxic ribonuclease alpha-sarcin to determine the binding sites for *Escherichia coli* ribosomal proteins L5, L18, and L25 on 5S rRNA. *Proc Natl Acad Sci USA 81*:322–326.

Goringer HU, Wagner R. 1986. Construction and functional analysis of ribosomal 5S RNA from *Escherichia coli* with single base changes in the ribosomal protein binding sites. *Biol Chem Hoppe-Seyler 367*:769–780.

Green R, Noller HF 1997. Ribosomes and translation. *Annu Rev Biochem 66*:679–716.

Ippolito JA, Steitz TA. 1998. A 1.3-Å resolution crystal structure of the HIV-1 *trans*-activation response region RNA stem reveals a metal ion-dependent bulge conformation. *Proc Natl Acad Sci USA 95*:9819–9824.

Ippolito JA, Steitz TA. 2000. The structure of the HIV-1 RRE high affinity rev binding site at 1.6 Å resolution. *J Mol Biol 295*:711–717.

Jaffrey SR, Haile DJ, Klausner RD, Harford JB. 1993. The interaction between the iron-responsive element binding protein and its cognate RNA is highly dependent upon both RNA sequence and structure. *Nucleic Acids Res 21*:4627–4631.

Jang SB, Hung LW, Chi YI, Holbrook EL, Carter RJ, Holbrook SR. 1998. Structure of an RNA internal loop consisting of tandem C-A^+ vase pairs. *Biochemistry 37*:11726–11731.

Joshua-Tor L, Frolow F, Apella E, Hope H, Rabinovich D, Sussman, JL. 1992. Three dimensional structures of bulge-containing DNA fragments. *J Mol Biol 225*:397-431.

McBryant SJ, Veldhoen N, Gedulin B, Leresche A, Foster MP, Wright PE, Romaniuk PJ, Gottesfeld JM. 1995. Interaction of the RNA binding fingers of *Xenopus* transcription factor IIIA with specific regions of 5S ribosomal RNA. *J Mol Biol 248*:44–57.

Meier N, Goringer HU, Keleuvers B, Scheibe U, Ebrtle J, Szymkowiak C, Zacharias M, Wagner R. 1986. The importance of individual nucleotides for the structure and function of rRNA in *E. coli. FEBS Lett 204*:89–95.

Navaza J. 1994. AMoRe: An automated package for molecular replacement. *Acta Cryst D50*:157–163.

Otwinowski Z, Minor W. 1997. Processing of X-ray diffraction data collected in oscillation mode. *Methods Enzymol 276*:307–326.

Pan B, Mitra SN, Sundaralingam M. 1998. Crystal structure of a 16-mer RNA duplex $r(GCAGAGUUAAAUCUGC)_2$ with wobble CCA^+ mismatches. *J Mol Biol 283*:977–984.

Pan B, Mitra SN, Sundaralingam M. 1999. Crystal structure of an RNA 16-mer duplex $r(GCAGAGUUAAAUCUGC)_2$ with nonadjacent G(syn).A^+(anti) mispairs. *Biochemistry 38*:2826–2831.

Parkinson G, Vojtchovsky J, Clowney L, Brunger AT, Berman HM. 1996. New parameters for the refinement of nucleic acid containing structures. *Acta Cryst D52*:57–64.

Pelham HRB, Brown DD 1980. A specific transcription factor that can bind either the 5S RNA gene or 5S RNA. *Proc Natl Acad Sci USA 77*:4170–4174.

Picard B, Wegnez M. 1979. Isolation of a 7S particle from *Xenopus laevis* oocytes: A 5S RNA–protein complex. *Proc Natl Acad Sci USA 76*:241–245.

Portmann S, Grimm S, Workman C, Usman N, Egli M. 1996. Crystal structures of an A-form duplex with single adenosine bulges and a conformational basis for site-specific RNA self-cleavage. *Chem Biol 3*:173–184.

Portmann S, Usman N, Egli M. 1995. The crystal structure of r(C-CCCGGGG) in two distinct lattices. *Biochemistry 34*:7569–7575.

Pritchard CE, Grasby JA, Hamy F, Zacharek AM, Singh M, Karn J, Gait MJ. 1994. Methylphosphonate mapping of phosphate contacts critical for RNA recognition by the human immunodeficiency virus tat and rev proteins. *Nucleic Acids Res 22*:2592–2600.

Rosett R, Monier R. 1963. A propos de la presence d'acide ribonucleique de faible poids moleculaire dans les ribosomes d'Escherichia coli. *Biochim Biophys Acta 68*:653–656.
Sergiev P, Dokudovskaya S, Romanova E, Tropin A, Bogdanov A, Brimacombe R, Dontsova O. 1998. The environment of 5S rRNA in the ribosome: Cross-links to the GTPase-associated area of 23S rRNA. *Nucleic Acids Res 26*:2519–2525.
Sharp PA. 1987. Splicing of messenger RNA precursors. *Science 235*:766–771.
Shatsky IN, Evstafieva AG, Bystrova TF, Bogdanov AA, Vasiliev VD. 1980. Topography of RNA in the ribosome: Location of the 3′-end of the 5S RNA on the central protuberance of the 50S subunit. *FEBS Lett 121*:97–100.
Shi K, Mitra SN, Biswas R, Sudaralingam M. 2000. The crystal structure of the octamer $[r(guauaca)dC]_2$ with six Watson–Crick base pairs and two 3′ overhang residues. *J Mol Biol 299*:113–122.
Shpanchenko OV, Zvereva MI, Dontsova OA, Nierhaus KH, Bogdanov AA. 1996. 5S rRNA sugar–phosphate backbone protection in complexes with specific ribosomal proteins. *FEBS Lett 394*:1–75.
Stoffler-Meilicke M, Stoffler G, Odom OW, Zinn A, Kramer G, Hardesty B. 1981. Localization of 3′-ends of 5S and 23S rRNAs in reconstituted subunits of *Escherichia coli* ribosomes. *Proc Natl Acad Sci USA 78*:5538–5542.
Sudarsanakumar C, Xiong Y, Sudaralingam M. 2000. Crystal structure of an adenine bulge in the RNA chain of a DNA•RNA hybrid, d(CTCCTCTTC)•r(gaagagagag). *J Mol Biol 299*:103–112.
Szymanski M, Barciszewska MZ, Barciszewsky J, Erdmann VA.1999. 5S ribosomal RNA data bank. *Nucleic Acids Res 27*:158–160.
Tang RS, Draper DE. 1990. Bulge loops used to measure the helical twist of RNA in solution. *Biochemistry 29*:5232–5237.
Theunissen O, Rudt F, Guddat U, Mentzel H, Peiler T. 1992. RNA and DNA binging zinc fingers in *Xenopus* TFIIIA. *Cell 71*:679–690.
Valegard K, Murray JB, Stonehouse NJ, van den Worm S, Stockley PG, Liljas L. 1997. The three-dimensional structures of two complexes btween recombinant MS2 capsids and RNA operator fragments reveal sequence-specific protein-RNA interactions. *J Mol Biol 270*:724–738.
Wedekind JE, McKay DB. 1999. Crystal structure of a lead-dependent ribozyme revealing metal binding sites relevant to catalysis. *Nat Struct Biol 6*:261–268.
Westman E, Stromberg R. 1994. Removal of t-butyldimethylsilyl protection in RNA-synthesis. Triethylamine trihydrofluoride (TEA, 3HF) is a more reliable alternative to tetrabutylammonium fluoride (TBAF). *Nucleic Acids Res 12*:2430–2431.
Woese CR, Gutell RR. 1989. Evidence for several higher order structural elements in ribosomal RNA. *Proc Natl Acad Sci USA 86*:3119–3122.
Wu HN, Uhlenbeck OC. 1987. Role of a bulged A residue in a specific RNA–protein interaction. *Biochemistry 26*:8221–8227.
Xiong Y, Sundaralingam M 1998. Crystal structure and conformation of a DNA-RNA hybrid duplex with a polypurine RNA strand: d(TTCTTBr5CTTC)-r(GAAGAAGAA). *Structure 6*:1493–1501.
Zacharias M, Hagerman PJ. 1995. Bulge-induced bends in RNA: Quantification by transient electric birefringence. *J Mol Biol 247*:486–500.
Zhang P, Popienick P, Moore PB. 1989. Physical studies of 5S RNA variants at position 66. *Nucleic Acids Res 17*:8645–8656.